Classical

Thin-Airfoil Theory

Enrique Ortega

eortega@cimne.upc.edu

Preliminary: vortex filaments and vortex sheets (I)

- As an extension of the point vortex, imagine an ***infinite straight vortex filament***, of strength Γ, which in any perpendicular plane induces the same field as a point vortex (i.e. the latter is simply a section of the vortex filament).

- Then, a **vortex sheet** may be thought as an infinite number of vortex filaments, each of which has infinitesimal strength and extends to infinite or to a boundary of the flow. For this arrangement, the local ***vortex sheet strength*** γ (or circulation density) is defined by

$$\gamma = \lim_{\Delta s \to 0} \left(\frac{1}{\Delta s} \oint \mathbf{V} \cdot d\boldsymbol{s} \right) \qquad (1)$$

  where Δs is the width of the sheet enclosed by the evaluation contour.

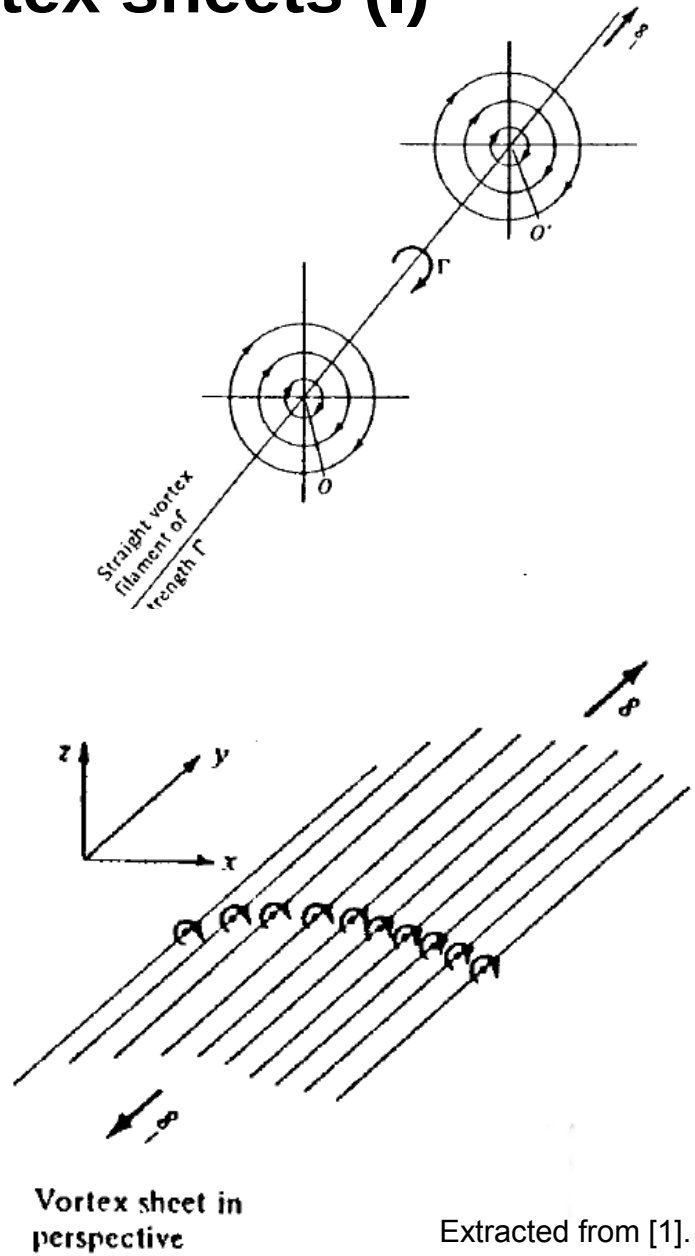

Vortex sheet in perspective

Extracted from [1].

Taking an elemental section of the vortex sheet, the velocity induced at a point **P** can be written as

$$dV = -\frac{\gamma ds}{2\pi r} \qquad \text{(normal to } r\text{)} \qquad (2)$$

Similarly to a point vortex, the resulting velocity field satisfies continuity and it is irrotational (except at the sheet itself). In addition, the velocity field is finite and continuous at any point of the flow. Near the vortex sheet we can state

$$\Gamma = \bar{\gamma}\Delta s = \oint \mathbf{V}\cdot d\boldsymbol{s} = u_1\Delta s - v_2\Delta n - u_2\Delta s + v_1\Delta n$$
$$= (u_1 - u_2)\Delta s + (v_1 - v_2)\Delta n$$

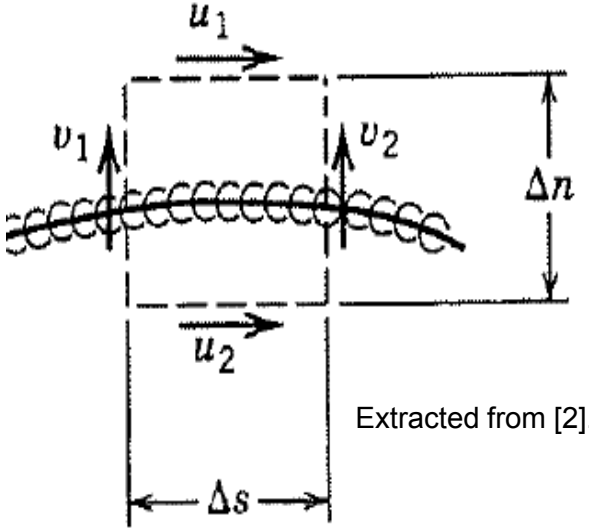

Extracted from [2].

where $\bar{\gamma}$ is an averaged strength. When $\Delta s \to 0$, v_1 and v_2 become identical, so that $(v_1 - v_2) \to 0$ (normal component is continuous). Furthermore, if $\Delta n \to 0$ then

$$\gamma(s) = u_1 - u_2 \qquad (3)$$

i.e. the local strength of the sheet is equal to the jump in the tangential velocity.

As the velocity field due to a vortex sheet satisfies continuity and is irrotational (and decays away from the airfoil satisfying the uniform flow condition), the solution of the airfoil problem can be reduced to find the circulation γ(s) which makes the airfoil contour to be a streamline of the flow (+Kutta condition!).Then,

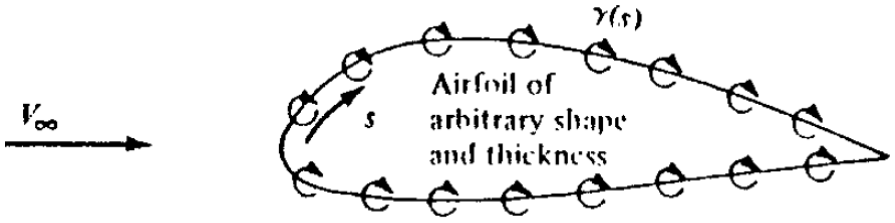

Extracted from [1].

$$\Gamma = \int \gamma \, ds$$

$$l = \rho_\infty V_\infty \Gamma$$

However, for arbitrary shape airfoils **no analytical solution exists for γ(s)** and this approach could not be solved until numerical computation allowed the introduction of panel methods. For the time being, some simplifications will be introduced for its solution.

It is interesting to note that vortex sheets placed along the airfoil contour can mimic to some extent the real flow behavior, because the resulting vorticity can be assimilable to that generated by viscosity inside the boundary layer. Some approaches for modeling viscous effects in potential flows follow this idea.

The thin-airfoil approximation

- If the **thickness is small** (usually t/c<15%), its effects can be neglected (when focusing on lift!) and the vortex sheet can be placed along the camber line.
- In addition, if the **camber is also small** (usually f/c<4%), the vorticity distribution $\gamma(s)$ can be placed along the chord line (planar wing approximation). Hence, $\gamma = \gamma(x)$.
- For such arrangement, the boundary conditions are similar as before: the mean camber line is a streamline of the flow (but with some simplification) and the Kutta condition is enforced at the trailing edge; i.e. $\gamma(TE)=0$. The latter avoids having infinite velocity at the edge of the vortex sheet.

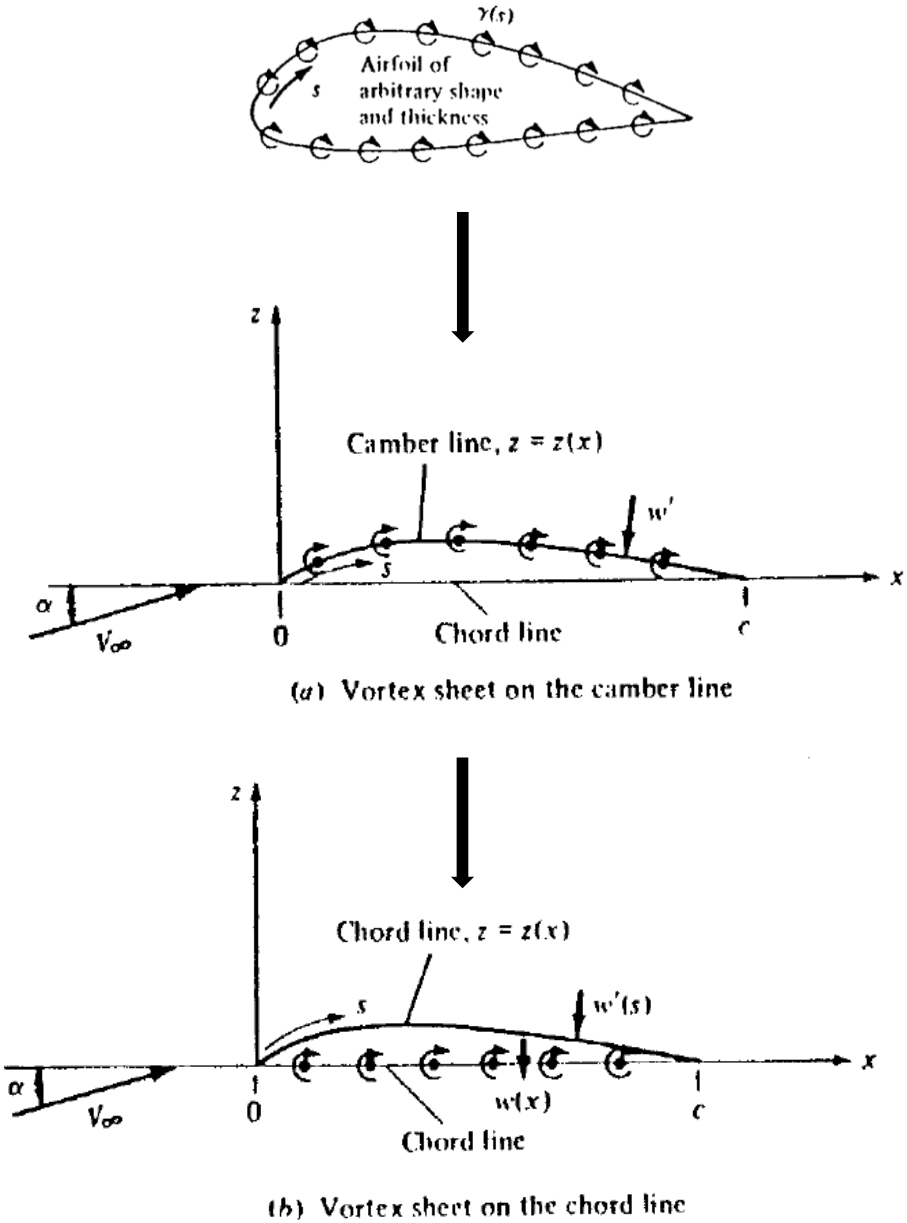

Extracted from [1].

Problem statement

If the mean camber line is a streamline of the flow, at any point **P** along z(x) we have

$$V_i^n + V_\infty^n = 0 \qquad (4)$$

where V_i^n is the normal component of the total velocity induced at **P** by the elemental circulations on the sheet, i.e.

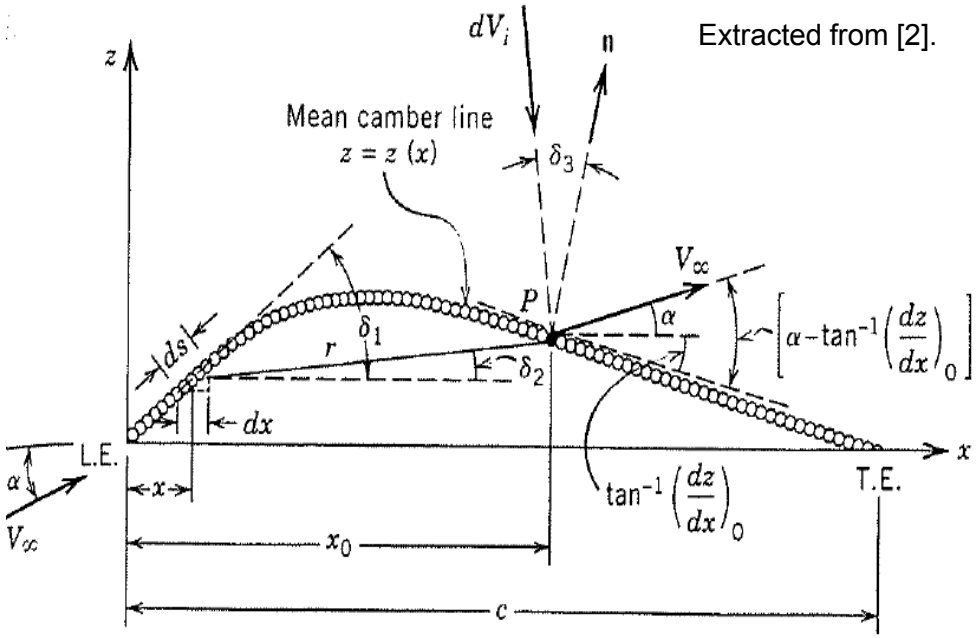

$$dV_i^n = -\frac{\gamma(x)ds}{2\pi r}\cos\delta_3 \;\Rightarrow\; V_i^n = -\frac{1}{2\pi}\int_0^c \frac{\gamma(x)\,ds}{r}\cos\delta_3 = -\frac{1}{2\pi}\int_0^c \frac{\gamma(x)\,dx}{x_0 - x}\frac{\cos\delta_2\cos\delta_3}{\cos\delta_1} \qquad (5)$$

and V_∞^n is the normal component of the freestream velocity at **P**, i.e.

$$V_\infty^n = V_\infty \sin\left[\alpha - \tan^{-1}\frac{dz}{dx}\right] \qquad (6)$$

Using Eqs. (5) and (6), the streamline boundary condition (4) results

$$\frac{1}{2\pi}\int_0^c \frac{\gamma(x)dx}{x_0 - x}\frac{\cos\delta_2\cos\delta_3}{\cos\delta_1} = V_\infty \sin\left[\alpha - \tan^{-1}\frac{dz}{dx}\right] \qquad (7)$$

which must be complemented with the Kutta condition

$$\gamma(TE) = 0 \qquad (8)$$

As the camber is small, we can assume that $\cos\delta_1 \approx \cos\delta_2 \approx \cos\delta_3 \approx 1$. In addition, if the angle of attack is also small, $\sin\alpha \approx \tan\alpha \approx \alpha$ (in rad). Then, Eq. (7) results

$$\frac{1}{2\pi}\int_0^c \frac{\gamma(x)dx}{x_0 - x} = V_\infty \left[\alpha - \tan^{-1}\frac{dz}{dx}\right] \qquad (9)$$

which is the **fundamental equation of the thin-airfoil theory**. The solution of the problem consists in solving Eq. (9) for γ(x) subject to Kutta condition (Eq. (8)).

Note that Eq. (9) is an integral equation which has a singularity at $x = x_0$. Thus, the principal value (finite part) of the integral is taken (see Appendix C in [3]).

Case of analysis I: symmetric airfoils

For convenience, the following transformation of coordinates is firstly introduced

$$x = c/2\,(1-\cos\theta)$$
$$dx = c/2\,\sin\theta d\theta \qquad (10)$$
$$\rightarrow x_0 = c/2\,(1-\cos\theta_0)$$

Extracted from [4].

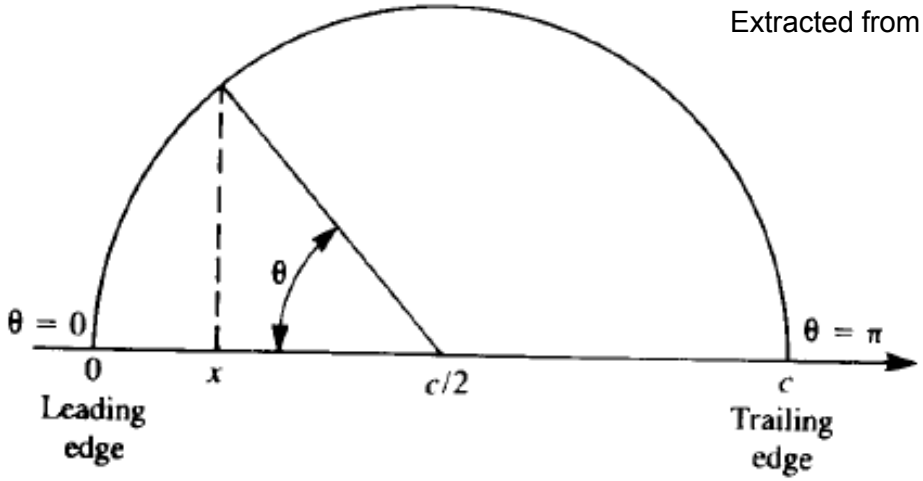

Then, the transformed thin-airfoil equations (8) and (9) can be written for the symmetric airfoil (dz/dx=0) as

$$\frac{1}{2\pi}\int_0^{\pi}\frac{\gamma(\theta)\sin\theta d\theta}{\cos\theta-\cos\theta_0} = V_\infty\alpha \qquad (11)$$

$$\gamma(\pi) = 0 \qquad (12)$$

It can be shown that a solution satisfying Eqs. (11) and (12) is

$$\gamma(\theta) = 2V_\infty \alpha \frac{1+\cos\theta}{\sin\theta} \qquad (13)$$

Hint: introduce Eq. (13) into Eq. (11) and use the result obtained for the Glauert's integral (see a demonstration in Appendix E of reference [4]), given by

$$\int_0^\pi \frac{\cos n\theta d\theta}{\cos\theta - \cos\theta_0} = \pi \frac{\sin n\theta_0}{\sin\theta_0} \quad n = 0,1,2,... \qquad (14)$$

For the The Kutta condition, introducing Eq.(13) into Eq. (12) we have

$$\gamma(\pi) = 2V_\infty \alpha \frac{1+\cos\pi}{\sin\pi} = 2V_\infty \alpha \frac{0}{0} \qquad \textit{indeterminate form}$$

Thus, applying L'Hopital's rule

$$\lim_{\theta\to\pi} \gamma(\theta) = 2V_\infty \alpha \left.\frac{-\sin\theta}{\cos\theta}\right|_{\theta=\pi} = 2V_\infty \alpha\,(0) = 0$$

Once $\gamma(\theta)$ is determined, the total circulation can be computed by

$$\Gamma = \int_0^c \gamma(x)dx = \int_0^\pi \gamma(\theta)\sin\theta d\theta = \pi\alpha V_\infty c \qquad (15)$$

and using the Kutta-Joukowsky theorem ($l=\rho_\infty V_\infty \Gamma$), the lift coefficient (per unit span) results

$$C_l = 2\pi\alpha \qquad (16)$$

where 2π is the lift slope. The moment coefficient can be obtained as follows

$$M_{LE} = -\int_0^c x\, dL = -\rho_\infty V_\infty \int_0^c x\, d\Gamma$$

$$= -\rho_\infty V_\infty \int_0^c x\,\gamma(x)dx \qquad (17)$$

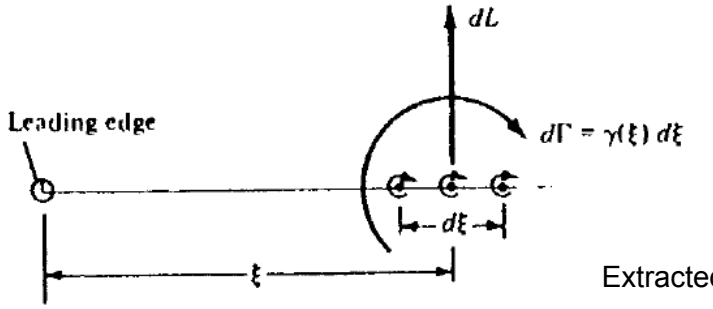

Extracted from [1].

Then, using the transformation (10) it is possible to obtain

$$C_{m_{LE}} = -\frac{\pi}{2}\alpha = -\frac{C_l}{4} \qquad (18)$$

From the definition of the center of pressure, we can state

$$\frac{x_{cp}}{c} \cong -\frac{C_{m_{LE}}}{C_l} = -\frac{(-C_l/4)}{C_l} = \frac{1}{4} \qquad (19)$$

Therefore, the moment about c/4 = constant = 0. Hence, $\mathbf{x_{ac} = x_{cp} = ¼\ c}$.

Remarks:

- The lift is proportionally linear to the angle of attack. Lift slope = const. = 2π (1/rad) $\approx$ 0.11 (1/deg).
- As expected, the angle of zero lift is $\alpha_{L0} = 0$.
- The moment (e.g. about the LE) is also linear with the angle of attack (or lift).
- The center of pressure (M=0) is located at a quarter chord point (c/4).
- The aerodynamic center (M does not depend on alpha) is coincident with the center of pressure. The Cm_{ac} (or Cm_0) is zero for symmetric airfoils.

Although the Cp distribution cannot be computed because thickness was neglected, the difference of pressure across the mean line can be obtained, e.g. taking the lift per unit area generated. Alternatively, from Eq. (3) we can state

$$\gamma(x) = V_U - V_L \quad \rightarrow \quad V_U \approx V_\infty + \tfrac{1}{2}\gamma(x)$$
$$V_L \approx V_\infty - \tfrac{1}{2}\gamma(x)$$

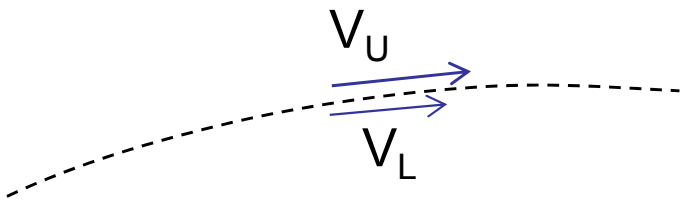

Then, using Bernoulli's equation for two points above and below the vortex sheet we can state

$$p_U + \tfrac{1}{2}\rho V_U^2 = p_L + \tfrac{1}{2}\rho V_L^2 V_U$$

and the jump in Cp results

$$\Delta Cp = \frac{p_L - p_U}{q_\infty} = 2\frac{\gamma(x)}{V_\infty} = \frac{2}{V_\infty}\left(2\alpha V_\infty \sqrt{\frac{c-x}{x}}\right)^{(*)}$$

$$= 4\alpha\sqrt{\frac{c-x}{x}} \qquad (20)$$

(*) Hint: use Eq. (13) with the transformation (10) and the following half-angle formulae

$$\tan\left(\frac{\theta}{2}\right) = \frac{\sin\theta}{1+\cos\theta} = \pm\sqrt{\frac{1-\cos\theta}{1+\cos\theta}}$$

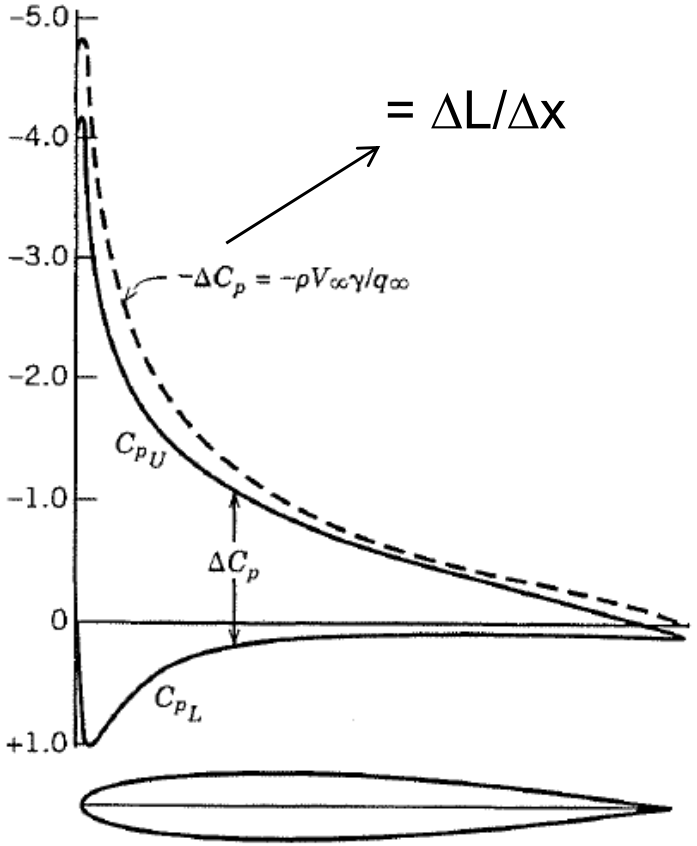

Fig. 5.7. Distribution of pressure coefficient and ΔC_p on NACA 0012 airfoil at $\alpha = 9°$.

Note that Eq. (20) is singular at the LE. This causes an error when evaluating the forces through integration of the pressure distribution. The contribution of the leading edge suction force can be computed by alternative methods, see for instance [3].

Example: NACA 0006 airfoil

Experimental values (*Re* = 3-9E6)

alpha	C_l
-4.0	-0.45
4.0	0.45

$$\frac{\partial C_l}{\partial \alpha} \cong 0.112$$

Note that for this airfoil the lift curve loses it linearity about 8 deg. In general, the scope of the ideal theory must be restricted to low alpha. Typically, for α > 8-10 deg viscous effects are not negligible, and the ideal flow model loses accuracy (α limits depend on Re, Mach and the airfoil geometry).

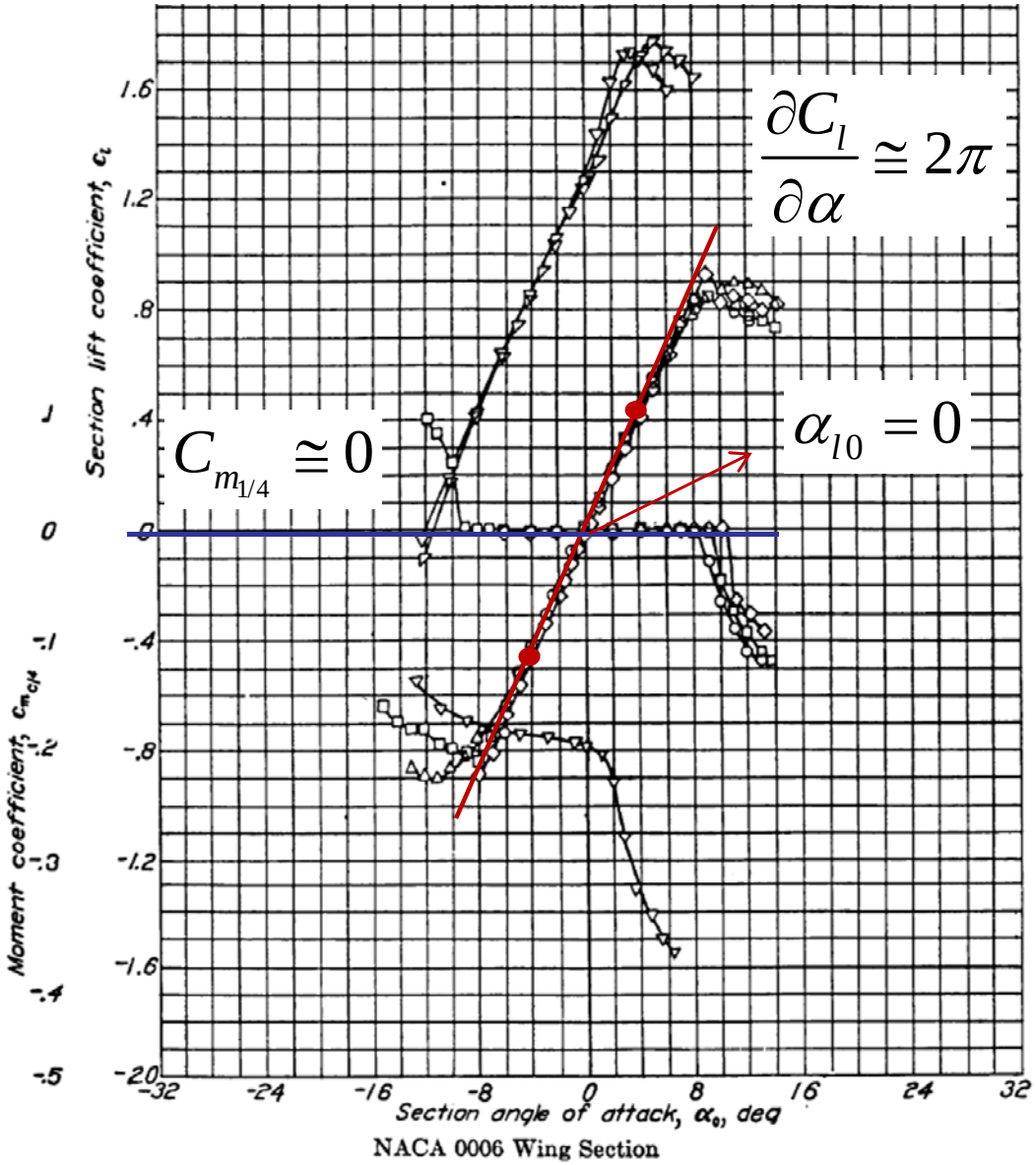

Extracted from [5].

Case of analysis II: cambered airfoil

The thin-airfoil equations to be solved are (see Eqs. (8) and (9))

$$\frac{1}{2\pi}\int_0^{\pi}\frac{\gamma(\theta)\sin\theta d\theta}{\cos\theta-\cos\theta_0}=V_\infty\left(\alpha-\frac{dz}{dx}\right) \qquad (21)$$

$$\gamma(\pi)=0 \qquad (22)$$

where x = c/2(1-cosθ) and 0≤θ≤π. A vorticity distribution satisfying these equations can be expressed as

$$\gamma(\theta)=2V_\infty\left[A_0\frac{1+\cos\theta}{\sin\theta}+\sum_{n=1}^{\infty}A_n\sin n\theta\right] \qquad (23)$$

In Eq. (23), the leading term is very similar to Eq. (13) and accounts for alpha and camber effects. The second term is a Fourier series summation, that accounts for camber effects, where the coefficients A_0, A_1,... must be determined to fulfill Eq. (21). Note that Eq. (22) is satisfied by the definition of Eq. (23).

Introducing Eq. (23) into the streamline condition given by Eq. (21)

$$\frac{\mathrm{A}_0}{\pi}\int_0^{\pi}\frac{1+\cos\theta}{\cos\theta-\cos\theta_0}d\theta+\sum_{n=1}^{\infty}\frac{\mathrm{A}_n}{\pi}\int_0^{\pi}\frac{\sin n\theta\sin\theta}{\cos\theta-\cos\theta_0}d\theta=\alpha-\frac{dz}{dx} \qquad (24)$$

Recalling Glauert's integral (see Appendix E in [4])

$$\int_0^{\pi}\frac{\cos n\theta d\theta}{\cos\theta-\cos\theta_0}=\pi\frac{\sin n\theta_0}{\sin\theta_0} \qquad n=0,1,2,... \qquad (25)$$

$$\int_0^{\pi}\frac{\sin n\theta\sin\theta d\theta}{\cos\theta-\cos\theta_0}=-\pi\cos n\theta_0 \qquad \left(\sin n\theta\sin\theta d\theta=\frac{1}{2}[\cos(n-1)\theta-\cos(n-1)\theta]\right) \qquad (26)$$

Using the integrals above, Eq. (24) results

$$\mathrm{A}_0-\sum_{n=1}^{\infty}\mathrm{A}_n\cos n\theta_0=\alpha-\frac{dz}{dx} \qquad (27)$$

Eq. (27) can be also expressed as

$$\left(\alpha - \mathrm{A}_0\right) + \sum_{n=1}^{\infty} \mathrm{A}_n \cos n\theta_0 = \frac{dz}{dx} \qquad (28)$$

which is in the form of a Fourier cosine series expansion for dz/dx. In general form, the latter is

$$f(\theta) = \mathrm{B}_0 + \sum_{n=1}^{\infty} \mathrm{B}_n \cos n\theta \quad 0 \le \theta \le \pi \quad (29) \quad \text{with} \quad \begin{cases} B_0 = \frac{1}{\pi}\int_0^{\pi} f(\theta)d\theta \\ B_n = \frac{2}{\pi}\int_0^{\pi} f(\theta)\cos n\theta d\theta \end{cases}$$

Then, assuming $f(\theta)=dz/dx$, by analogy of Eqs. (28) and (29), the A_n coefficients (satisfying the streamline condition) result

$$A_0 = \alpha - \frac{1}{\pi}\int_0^{\pi} \frac{dz}{dx} d\theta_0 \quad ; \quad A_n = \frac{2}{\pi}\int_0^{\pi} \frac{dz}{dx} \cos n\theta_0 d\theta_0 \qquad (30)$$

Hence, Eq. (23) can be solved for a given airfoil and angle of attack by using the coefficients (30). Note that $\gamma(\theta)$ reduces to the symmetric case (Eq.(13)) if $^{dz}/_{dx}=0$ ($A_0=\alpha$). The leading terms $A_{1,2,...}$ depend only of the shape of the mean line.

The contribution of A_0 and the A_n terms to the circulation are sketched below

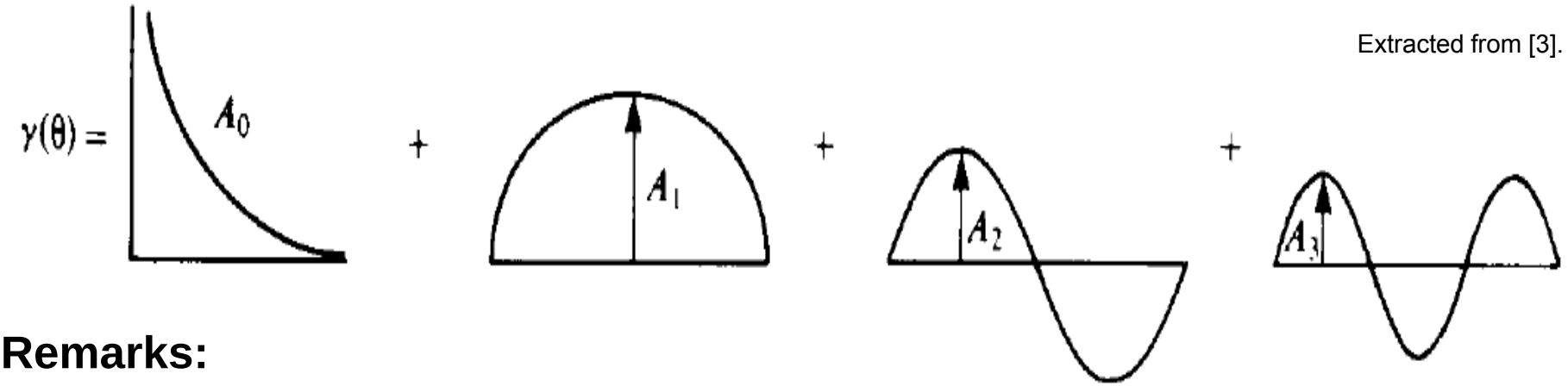

Extracted from [3].

Remarks:

- The terms A_0, A_1, A_2,… satisfy the Kutta condition at the trailing edge.
- The terms A_n form a trigonometric expansion with enough capability to reproduce an arbitrary distribution of circulation.
- The term A_0 provides more weight to the leading edge zone (where a high suction area is expected). Note that A_0 is higher in that zone and goes to zero towards the trailing edge.
- The purpose of the constant $2V_\infty$ introduced in $\gamma(\theta)$ is simply to cancel the $2V_\infty$ term in the right-hand-side of Eq. (21).

The total circulation can be obtained by

$$\Gamma = \int_0^c \gamma(x)dx = \frac{c}{2}\int_0^\pi \gamma(\theta)\sin\theta d\theta \qquad (31)$$

Introducing Eq. (23) into Eq. (31)

$$\Gamma = cV_\infty \left[A_0 \underbrace{\int_0^\pi (1+\cos\theta)d\theta}_{\pi} + \sum_{n=1}^{\infty} A_n \underbrace{\int_0^\pi \sin n\theta \sin\theta d\theta}_{\pi/2 \text{ for } n=1 \text{ ; } 0 \text{ for } n\neq 1} \right]$$

the circulation results

$$\Gamma = cV_\infty \left(A_0\pi + A_1\frac{\pi}{2} \right) \qquad (32)$$

and using the Kutta-Joukowsky theorem ($l=\rho_\infty V_\infty \Gamma$), the lift coefficient (per unit span) results

$$C_l = \left(2A_0 + A_1\right)\pi \qquad (33)$$

Introducing Eqs. (30) into Eq. (33), the lift coefficient can be written as

$$C_l = 2\pi\left[\alpha + \frac{1}{\pi}\int_0^{\pi}\frac{dz}{dx}(\cos\theta_0 - 1)d\theta_0\right] \qquad (34)$$

It can be observed that, similarly to the symmetric case, the C_l varies linearly with α, with slope 2π (1/rad). Eq. (34) also shows that for cambered airfoils $C_l \neq 0$ at $\alpha=0$. Making Eq. (34) equal to zero, the angle of zero lift α_{L0} results

$$\alpha_{l=0} = \alpha_{l0} = -\frac{1}{\pi}\int_0^{\pi}\frac{dz}{dx}(\cos\theta_0 - 1)d\theta_0 \qquad (35)$$

Hence, the lift coefficient can be also expressed as

$$C_l = 2\pi(\alpha - \alpha_{l0}) \qquad (36)$$

where the term $(\alpha-\alpha_{l0})$ is the absolute angle of attack. Note that in general α_{l0} is negative.

A line parallel to V_∞, which passes through the TE making an angle α_{LO} with respect to the chord is called the *Zero-Lift-Line*. The airfoil generates zero lift moving in that direction. For symmetrical airfoils the ZLL is coincident with the chord line.

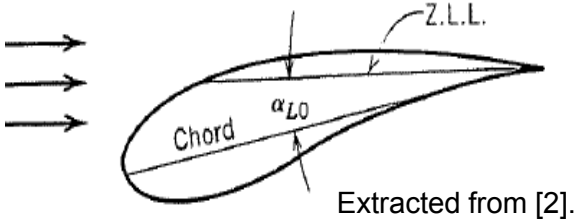

Extracted from [2].

The moment characteristics for a cambered airfoil can be obtained similarly to the symmetrical case by using Eq. (17). This procedure yields

$$C_{m_{LE}} = -\left(A_0 + A_1 - \frac{A_2}{2} \right) \frac{\pi}{2} \qquad (37)$$

Introducing Eq. (33) into Eq. (37), the moment coefficient can be written as

$$C_{m_{LE}} = -\frac{C_l}{4} + \left(A_2 - A_1 \right) \frac{\pi}{4} \qquad (38)$$

It is possible to note that the terms A_1 and A_2 in Eqs. (37) and (38) do not depend on α or C_l; therefore, they only contribute to the airfoil free moment Cm_0.

From the definition of center of pressure, for the cambered airfoil we have

$$\frac{x_{CP}}{c} = -\frac{C_{m_{LE}}}{C_l} = \frac{1}{4} + \frac{\pi}{4C_l}\left(A_1 - A_2\right) \qquad (39)$$

where it is possible to observe that x_{cp} varies with lift and tends to infinite when $C_l \rightarrow 0$ (these characteristics make x_{cp} useless for practical analyses). Taking moment with respect to the quarter chord point, it is possible to obtain

$$C_{m_{1/4}} = \left(A_2 - A_1\right)\frac{\pi}{4} \qquad (40)$$

which, as seen before, does not depend on alpha (A_1 and A_2 are only a function of the shape of the camber line). Hence, it can be concluded that the aerodynamic center for the cambered airfoil is located at $\mathbf{x_{ac} = x_{c/4}}$.

Summarizing, for cambered airfoils we have seen that

- Similar to the symmetrical case, the lift is proportionally linear to the angle of attack. The lift slope is constant = 2π (1/rad) $\approx$ 0.11 (1/deg).
- The angle of zero lift is different from zero ($\alpha_{L0} < 0$) and its value depends only on the shape of the mean line.
- The moment (e.g. about the LE) has two contributions: one due to Cm_0, which depends on the camber line and is constant, and another which is proportional to the angle of attack (or lift).
- The center of pressure (M=0) varies with lift. It is located at the quarter chord point (c/4) when Cl = 0, and tends to infinite when Cl$\rightarrow$0.
- Similar to symmetric airfoils, the aerodynamic center (M does not depend on alpha) is located at c/4. The Cm_{ac} (or Cm_0) depends on the shape of the mean line and it is generally a negative number.

Example: NACA 23012 airfoil

Comparison between theoretical and experimental data (*Re* = 3-9E6). *See [1], example 4.6, pp. 313.*

	Theoretical	Experimental
C_l @ α = 4º	0.559	0.55
α_{l0}	-1.09	-1.1
$Cm_{1/4}$	-0.0127	-0.01

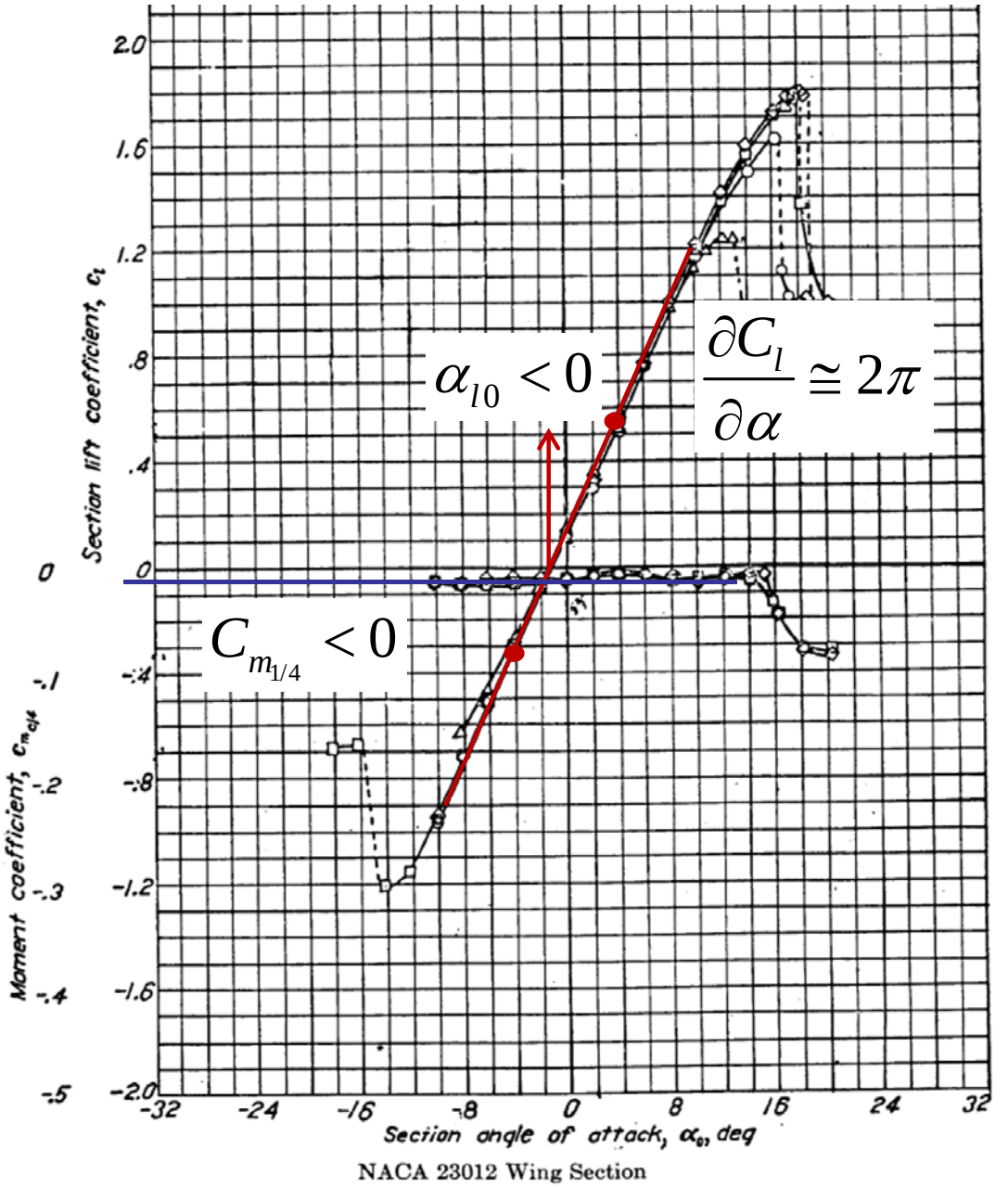

NACA 23012 Wing Section

Extracted from [5].

Effects of camber on some aerodynamic variables

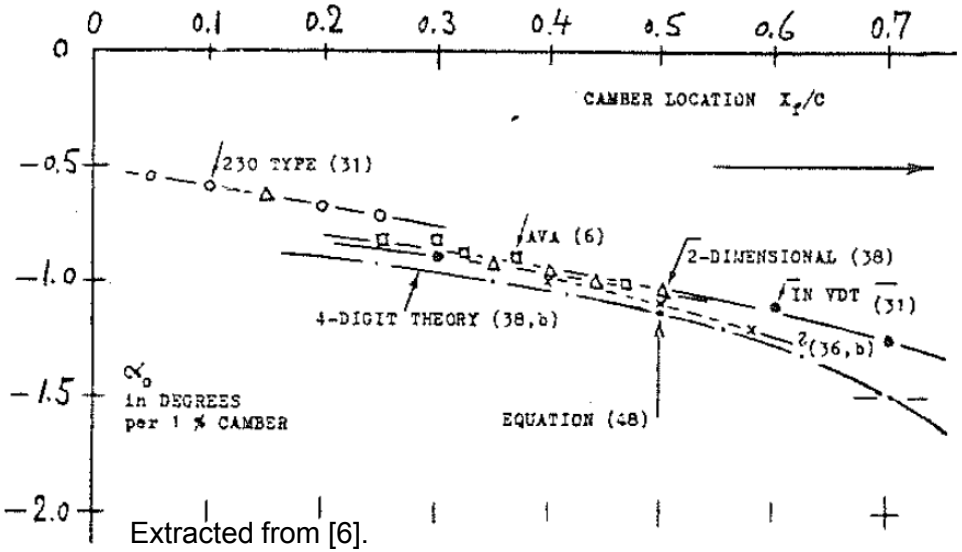

Extracted from [6].

Figure 25. Angle of attack for zero lift, for camber ratios up to 2 or 3%, as a function of the location of camber along the section chord.

Extracted from [2].

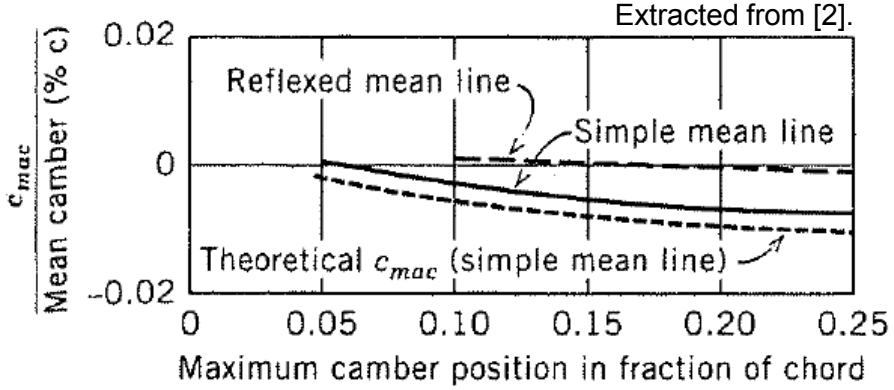

Extracted from [6].

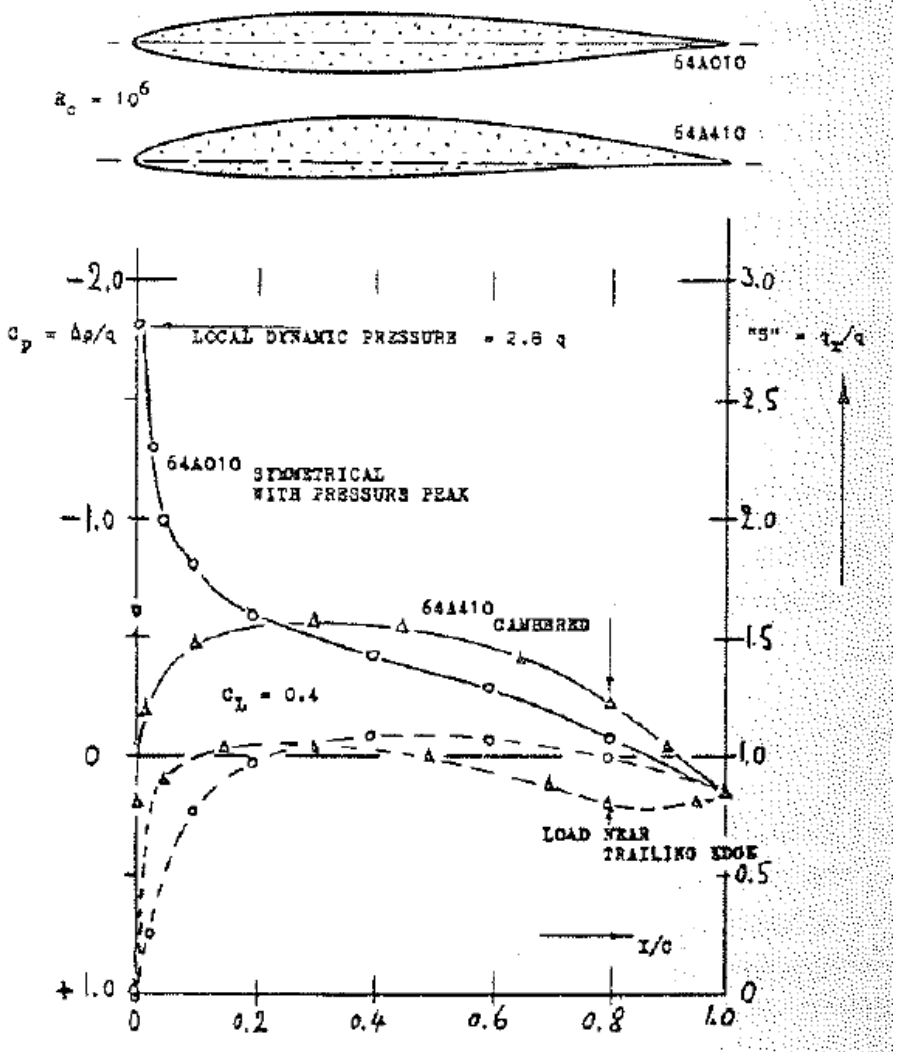

Figure 26. The pressure distribution of a properly cambered, in comparison to that of a symmetrical airfoil section (53,e).

Case of analysis III: extension to trailing edge flaps

- As seen before, for a general cambered airfoil the distribution of circulation can be decomposed into a component due to a flat plate (c) with angle of attack, and a component depending on the shape of the camber line (a).
- Similarly, profiting from the linearity of the problem, the effect of trailing edge devices can be studied by an additional camber of the mean line caused by deflection of the flap (b). Thus, its circulation can be added to the previous ones in order to obtain the result sought (a+b+c).

The next analysis focuses particularly on plain-type trailing edge flaps.

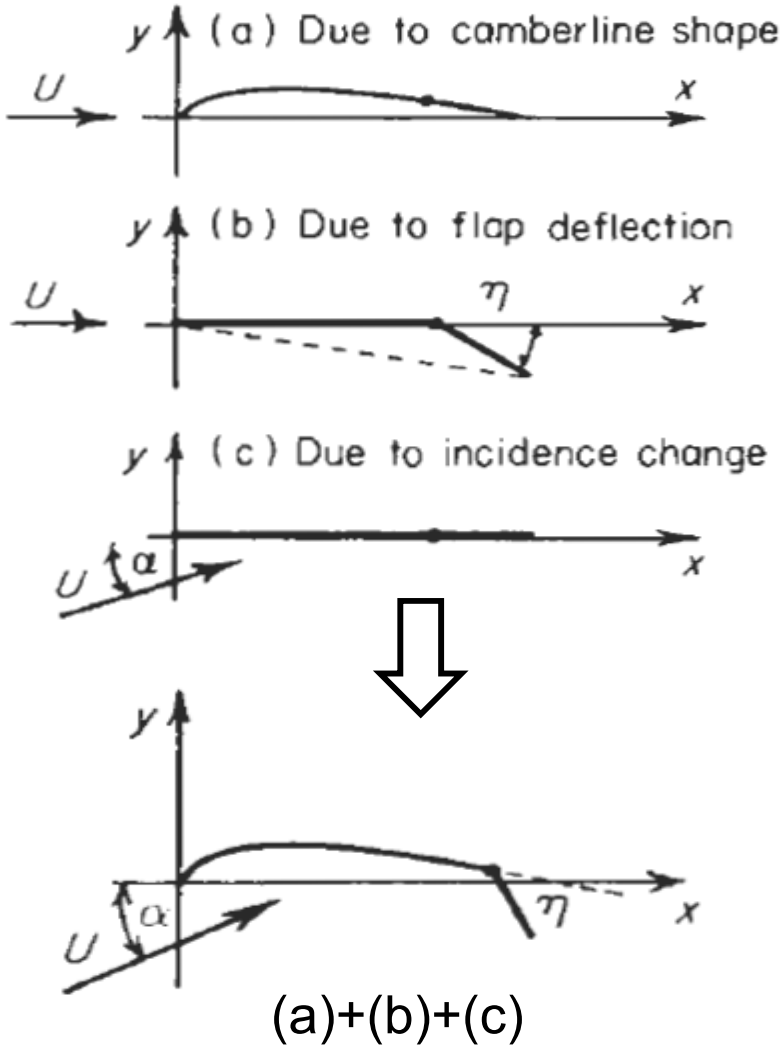

(a)+(b)+(c)

Extracted from [7].

Profiting from the linearity of the problem, we can write

$$C_l = \frac{\partial C_l}{\partial \alpha}\left(\alpha - \alpha_{l0}\right) + \frac{\partial C_l}{\partial \eta}\eta$$

$$= \frac{\partial C_l}{\partial \alpha}\left(\alpha - \alpha_{l0}\right) + \frac{\partial C_l}{\partial \alpha}\frac{\partial \alpha}{\partial \eta}\eta \qquad (41)$$

where all the angles are small and the viscous effects are assumed to be negligible. Then, since the angle of attack α is not affected by flap deflection, Eq. (41) results

$$C_l = \frac{\partial C_l}{\partial \alpha}\left[\alpha - \left(\alpha_{l0} + \underline{\frac{\partial \alpha_{l0}}{\partial \eta}\eta}\right)\right] \qquad (42)$$

The underlined term in Eq. (42) can be seen as a $\Delta\alpha_{l0}$, caused by flap deflection, which generates a lift increment ΔC_l. This quantity can be computed and added to the basic camber line solution (without flap) to obtain the solution of the airfoil with flap deflected.

Focusing on the effects of flap deflection on the zero-lift angle, from Eq. (35) we have that, for a general cambered airfoil

$$\alpha_{l0} = -\frac{1}{\pi}\int_0^{\pi} \frac{dz}{dx}(\cos\theta_0 - 1)d\theta_0 \quad \text{with} \quad 0 \le \theta_0 \le \pi \qquad (43)$$

As it is possible to observe, the term ($\cos\theta_0$-1) is zero at the LE and achieves it maximum when $\theta=\pi$, i.e. at the TE. This indicates that the part of the mean line near the TE has the highest impact on α_{l0}. The design of devices like trailing-edge flaps or ailerons is based on this fact.

Example: a downward deflection of the mean line near the TE makes α_{l0} more negative, hence increases the lift at the same geometrical α. Although α_{stall} is reduced with flap deflection, this reduction is lower than the gain achieved in lift, and Cl_{max} increases. The lift slope is not affected by flap deflection.

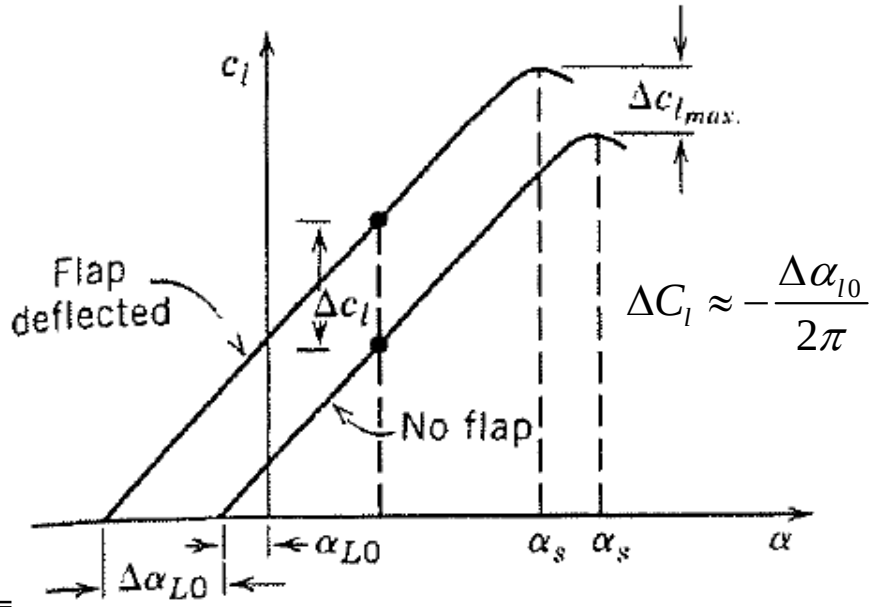

In order to compute the effect of the flap deflection, the following geometry is proposed

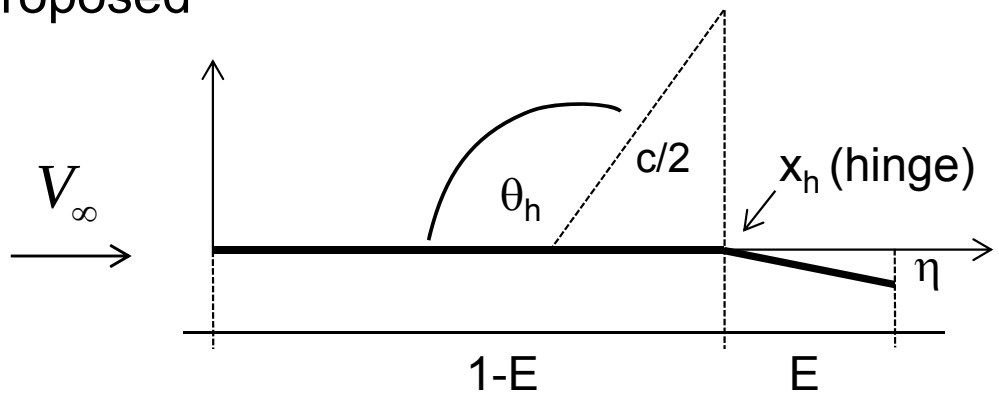

$$\frac{dz}{dx}\begin{cases} 0 & x/c \le 1-E \\ -\eta & x/c > 1-E \end{cases}$$

with E = 1-x_h/c (flap-chord ratio)
and tan η ≈ η

The α_{l0} term can be evaluated from Eq. (43) as follows

$$\alpha_{l0} = -\frac{1}{\pi}\int_0^\pi \frac{dz}{dx}(\cos\theta_0 - 1)d\theta_0 = -\frac{1}{\pi}\left[\int_0^{\theta_h} \ldots + \int_{\theta_h}^{\pi} \ldots\right]$$

(dz/dx=0)

$$= -\frac{1}{\pi}\int_{\theta_h}^{\pi}(-\eta)(\cos\theta_0 - 1)d\theta_0 \quad \Rightarrow \alpha_{l0} = -\frac{\eta}{\pi}\left(\pi - \theta_h + \sin\theta_h\right) \qquad (44)$$

Then, the incremental variation of the zero-lift angle due to flap deflection is

$$\Delta\alpha_{l0} = \frac{\partial\alpha_{l0}}{\partial\eta}\eta = -\left(1 - \frac{\theta_h}{\pi} + \frac{\sin\theta_h}{\pi}\right)\eta \qquad (45)$$

$\partial\alpha_{l0}/\partial\eta$ is usually called the *flap efficiency factor.*

From Eq. (42), using Eq. (45) the incremental lift results

$$\Delta C_l = -2\pi\Delta\alpha_{l0} = 2\left(\pi - \theta_h + \sin\theta_h\right)\eta \qquad (46)$$

The change in the moment coefficient can be evaluated in a similar manner. For example, using Eq. (40) we can write

$$C_{m_{1/4}} = \left(A_2 - A_1\right)\frac{\pi}{4} = \frac{1}{2}\left(\int_0^\pi \frac{dz}{dx}\cos 2\theta_0 d\theta_0 - \int_0^\pi \frac{dz}{dx}\cos\theta_0 d\theta_0\right)$$

$$= \frac{1}{2}\left(\int_{\theta_h}^\pi (-\eta)\cos 2\theta_0 d\theta_0 - \int_{\theta_h}^\pi (-\eta)\cos\theta_0 d\theta_0\right) \qquad (47)$$

and after integration Eq. (47) yields(*),

$$\Delta C_{m_{1/4}} = -\frac{1}{2}\sin\theta_h(1-\cos\theta_h)\,\eta \qquad (48)$$

As it can be observed in Eqs. (45), (46) and (48), the incremental values for α_{l0}, C_l and C_m vary linearly with the flap deflection η.

(*) Use the identity sin2A = 2·sinA·cosA

Computation of the hinge moment coefficient

The aerodynamic moment at the flap hinge can be computed by

$$M_h = -\int_{x_h}^{c} (x - x_h) dL = -\rho_\infty V_\infty \int_{x_h}^{c} (x - x_h)\, d\Gamma$$

$$= -\rho_\infty V_\infty \int_{x_h}^{c} (x - x_h)\, \gamma(x) dx \qquad (49)$$

Then, using the transformation (10) and dividing by $q_\infty c^2(1)$, the dimensionless form of Eq. (49) results

$$C_h = -\frac{1}{2V_\infty} \int_{\theta_h}^{\pi} (\cos\theta_h - \cos\theta)\gamma(\theta)\sin\theta d\theta$$

$$= -\int_{\theta_h}^{\pi} (\cos\theta_h - \cos\theta) \left[\mathrm{A}_0 \frac{1+\cos\theta}{\sin\theta} + \sum_{n=1}^{\infty} \mathrm{A}_n \sin n\theta \right] \sin\theta d\theta \qquad (50)$$

From Eqs. (30), the coefficients A_0 and A_n are

$$A_0 = \alpha - \frac{1}{\pi}\int_{\theta_h}^{\pi} \frac{dz}{dx} d\theta = \alpha + \eta\left(1 - \frac{\theta_h}{\pi}\right) \quad ; \quad A_n = \frac{2}{\pi}\int_{\theta_h}^{\pi} \frac{dz}{dx}\cos n\theta d\theta = -\eta\frac{2\sin n\theta_h}{n\pi}$$

and replacing into Eq. (49), the hinge moment coefficient can be written as

$$C_h = -\int_{\theta_h}^{\pi} (\cos\theta_h - \cos\theta)\left[\alpha + (1 - \frac{\theta_h}{\pi})\eta\right](1+\cos\theta)d\theta$$
$$+\int_{\theta_h}^{\pi} (\cos\theta_h \sin\theta - \cos\theta\sin\theta)\left[\eta\sum_{n=1}^{\infty}\frac{2\sin n\theta_h}{n\pi}\sin n\theta\right]d\theta \qquad (51)$$

Collecting terms we can obtain

$$C_h = -\alpha\left[\cos\theta_h\, \mathrm{I}_1 - \mathrm{I}_2\right]$$
$$-\eta\left[\left(1 - \frac{\theta_h}{\pi}\right)\left(\cos\theta_h\, \mathrm{I}_1 - \mathrm{I}_2\right) + \sum_{n=1}^{\infty}\frac{2\sin n\theta_h}{n\pi}\left(\cos\theta_h\, \mathrm{I}_3 - \mathrm{I}_4\right)\right] \qquad (52)$$

The integral terms $I_{1\text{-}4}$ in Eq. (52) are:

$$I_1 = \int_{\theta_h}^{\pi} (1+\cos\theta)d\theta = \pi - \theta_h - \sin\theta_h$$

$$I_2 = \int_{\theta_h}^{\pi} (1+\cos\theta)\cos\theta d\theta = \left[\sin\theta_h + \frac{\pi-\theta_h}{2} - \frac{\sin 2\theta_h}{4} \right]$$

$$I_3 = \int_{\theta_h}^{\pi} \sin n\theta \sin\theta d\theta = \frac{1}{2}\left[\frac{\sin(n+1)\theta_h}{n+1} - \frac{\sin(n-1)\theta_h}{n-1} \right]$$

$$I_4 = \int_{\theta_h}^{\pi} \sin n\theta \sin\theta \cos\theta d\theta = \frac{1}{2}\left[\frac{\sin(n+2)\theta_h}{n+2} - \frac{\sin(n-2)\theta_h}{n-2} \right]$$

Note that the hinge moment coefficient (52) is written in terms of the angle of attack (which can be put in terms of the lift) and the flap deflection. Thus, it is a common practice to express

$$C_h = \frac{\partial C_h}{\partial C_l} C_l + \frac{\partial C_h}{\partial \eta} \eta + C_{h0} \qquad (53)$$

where the theoretical derivatives usually include experimental corrections. The term C_{h0} in Eq. (53) is added to account for the moment caused by the basic form of the airfoil, which is not accounted for in this development.

Other comparisons with experimental results

I. Lift slope

$$\frac{\partial C_l}{\partial \alpha} \cong 0.107$$

Extracted from [5].

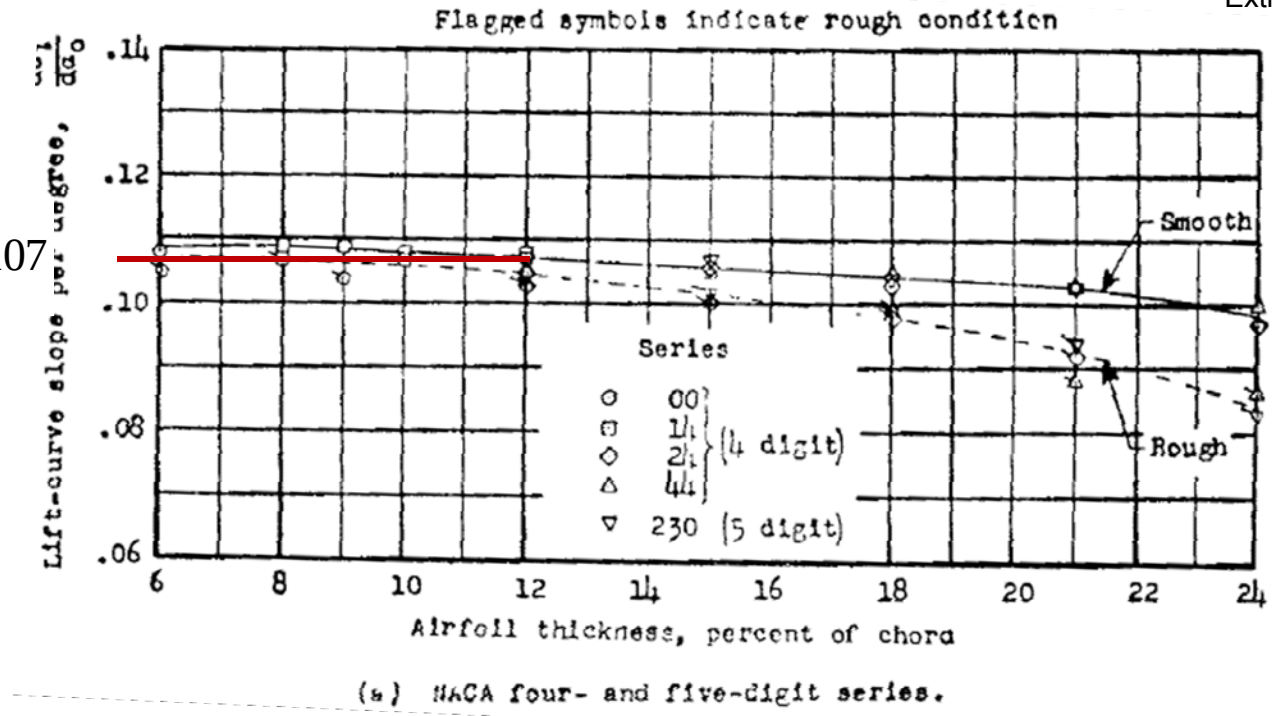

(a) NACA four- and five-digit series.

- For t/c ≤ 24%, the $C_{l,\alpha}$ predicted is within 15% of accuracy with respect to experimental values (but note that such thick airfoils are not very frequent in practice).
- For typical airfoils with **t/c about 12%, the accuracy is within 3%,** which is a very good approximation. Comparable results can be obtained for other airfoil families, see [5].

II. Aerodynamic center

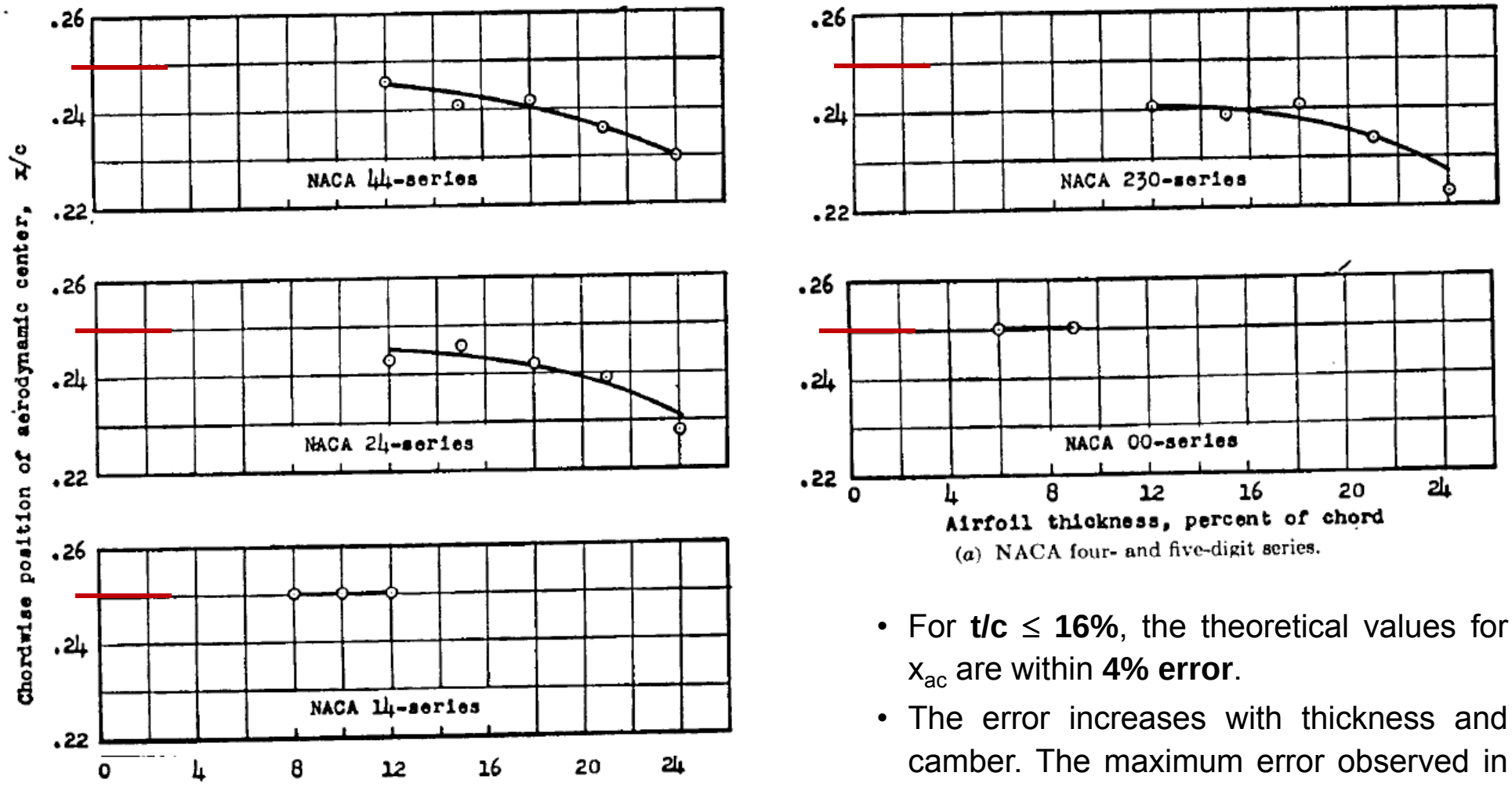

(a) NACA four- and five-digit series.

FIG. 94. Variation of section chordwise position of the aerodynamic center with airfoil thickness ratio for several NACA airfoil sections of different cambers. R, 6×10^6.

Extracted from [5].

- For **t/c ≤ 16%**, the theoretical values for x_{ac} are within **4% error**.
- The error increases with thickness and camber. The maximum error observed in the figures is about 12% (max. thickness).

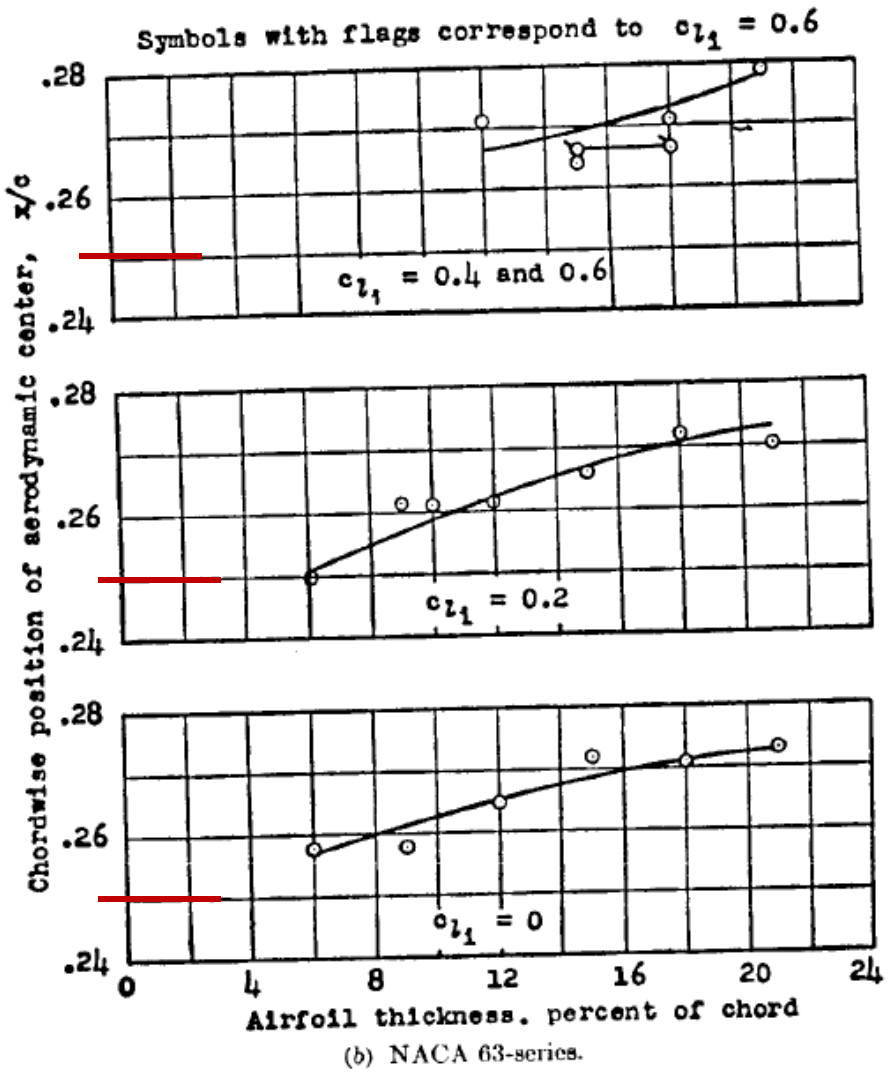

(b) NACA 63-series.

Extracted from [5].

- In the NACA 6-series, particularly for the thicker airfoils, the aerodynamic center is located aft the quarter chord point.
- The delayed chordwise position of the minimum Cp has an effect on x_{ac}.

A note on the vertical position of the AC

In real flows, the aerodynamic center is slightly above the chord line. The z coordinate can be found by enforcing linear behavior of the Cm and computing the deviation. The vertical position of the AC is computed to compensate this deviation. It can be found [6] that $z/c \approx -7\Delta Cm/Cl^2$.

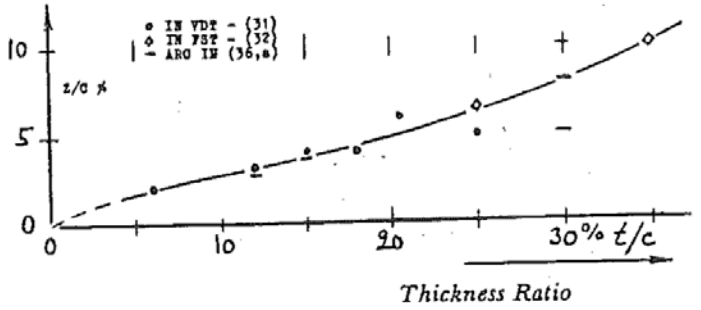

Figure 45. Vertical position of the aerodynamic center for various types of foil sections.

III. Flap deflection

Extracted from [5].

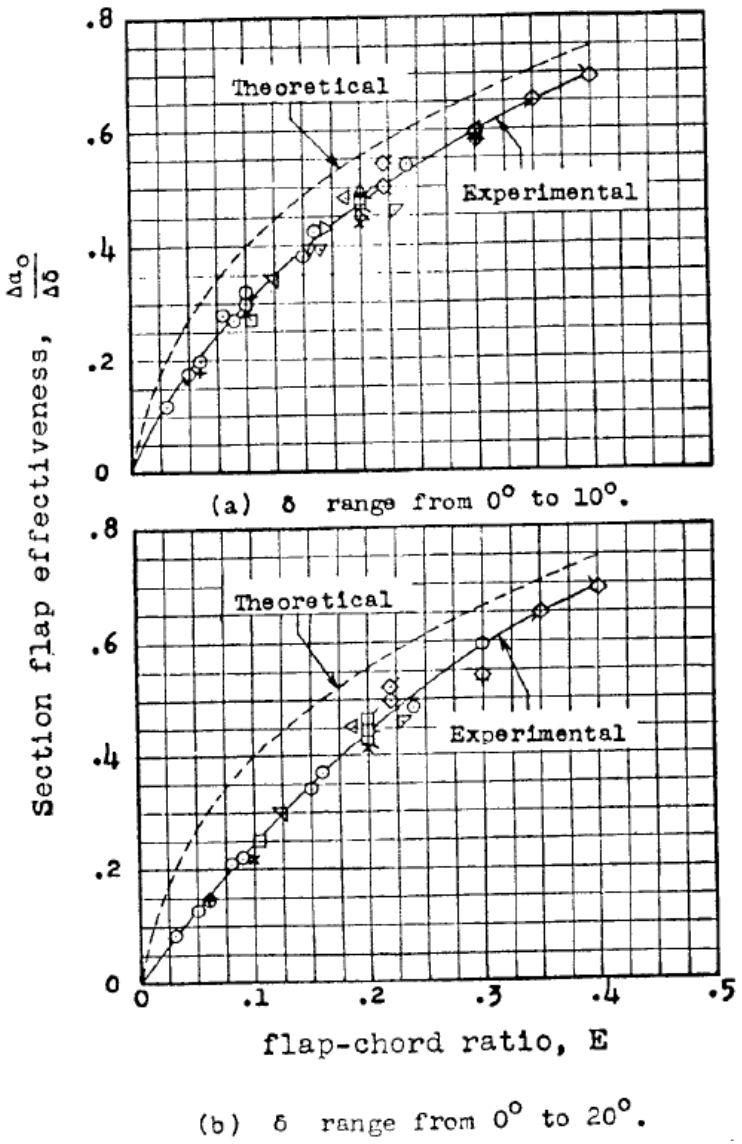

- When E is low, the relation between the boundary layer thickness and the flap size increases, thus the efficiency achieved in practice is reduced.
- As expected, the agreement with theory improves as E increases.

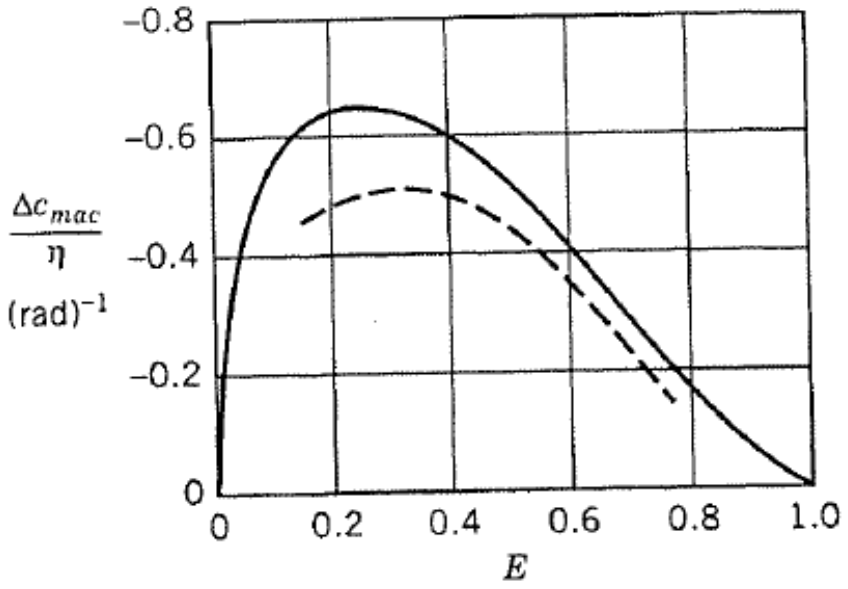

Extracted from [2].

In order to account for real flow effects, some empirical corrections are usually applied to the theoretical flap efficiency factor. For instance, the following correction is proposed in [8]

$$\left(\frac{\partial \alpha_{l0}}{\partial \eta}\right)_C = \left(\frac{\partial \alpha_{l0}}{\partial \eta}\right)_T \times factor \qquad (54)$$

where the subscripts C and T indicate corrected and theoretical results respectively, and *factor* is an experimental value obtained for different types of trailing edge devices (see Figure on the left).

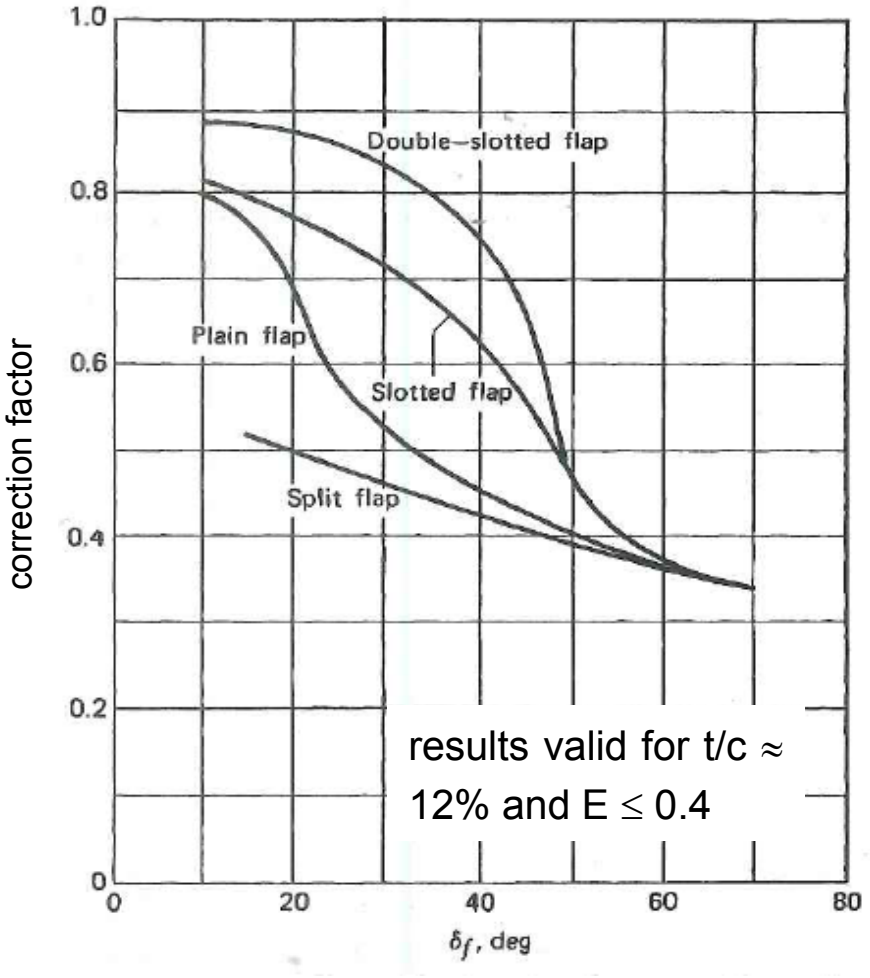

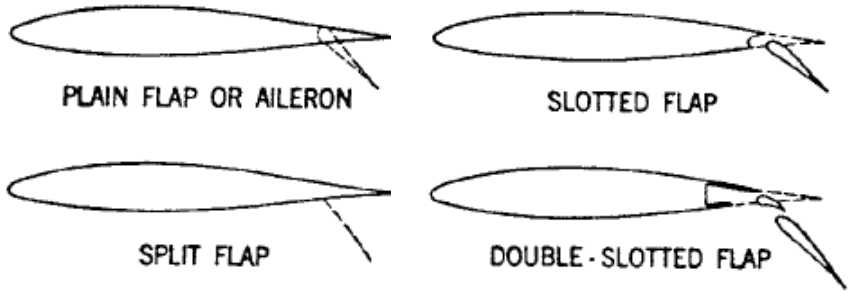

References

1. Anderson J. D. Jr. Fundamentals of aerodynamics, 3rd edition. McGraw-Hill Book Company (1984).
2. Kuethe, A. M., Chow, C. Y. Foundations of aerodynamics. Bases of aerodynamic design. 5th edition. John Wiley and Sons (1998).
3. Katz J., Plotkin A. Low speed aerodynamics: from wing theory to panel methods. McGraw-Hill series in aeronautical and aerospace engineering (1991).
4. Karamcheti K. Principles of ideal-fluid aerodynamics. R. E. Krieger Pub. Co (1980).
5. Abbott, I. H., Doenhoff, A. E. V. Theory of wing sections. Including a summary of airfoil data. New York: Dover (1959).
6. Hoerner, S. F., Borst, H. V. Fluid-dynamic lift: practical information on aerodynamic and hydrodynamic lift (1985).
7. Houghton, E. L., Carpenter, P. W. Aerodynamics for engineering students. 5th edition. Butterworth-Heinemann (2003).
8. McCormick, B. W. Aerodynamics, aeronautics, and flight mechanics. 2nd edition. John Wiley and Sons (1995).

Enrique Ortega
eortega@cimne.upc.edu